



Available online at www.sciencedirect.com

SCIENCE @ DIRECT[®]

Computers & Graphics 28 (2004) 895–906

COMPUTERS
& GRAPHICS

www.elsevier.com/locate/cag

Technical Section

PDE blending surfaces with C^2 continuity

L.H. You, P. Comninou, Jian J. Zhang*

The National Centre for Computer Animation, Talbot Campus, Bournemouth University, Weymouth House, Fern Barrow Poole,
Dorset BH12 5BB, UK

Abstract

In this paper, we propose to use a general sixth-order partial differential equation (PDE) to solve the problem of C^2 continuous surface blending. Good accuracy and high efficiency are obtained by constructing a compound solution function, which is able to both satisfy the boundary conditions exactly and minimise the error of the PDE. This method can cope with much more complex surface-blending problems than other published analytical PDE methods. Comparison with the existing methods indicates that our method is capable of generating blending surfaces almost as fast and accurately as the closed-form method and it is more efficient and accurate than other extant PDE-based methods.

© 2004 Published by Elsevier Ltd.

Keywords: Generation of blending surfaces; C^2 continuity; Sixth-order PDEs; Efficient and effective resolution method

1. Introduction

In engineering design and computer graphics, the problem of smoothly connecting two or more surfaces is known as surface blending and is of great importance.

A survey of existing literature reveals that the blending of two primary surfaces (expressed mainly in implicit or parametric form) has been widely investigated. It emerges that the potential method [1] by Ohkura and Kakazu et al. is the most widely used method for blending implicit surfaces.

Another important blending technique used with implicit surfaces is the rolling-ball method. It was first proposed by Rossignac and Requicha [2]. Using the rolling-ball method to blend implicit surfaces was investigated by Lukács [3] et al. The rolling-ball method was also widely applied to blending parametric surfaces. Depending on whether the radius of the rolling-ball

varies, rolling-ball blends are classified as constant-radius blends and variable-radius blends. The constant-radius rolling-ball method was studied by Barnhill et al. [4] and the others. Variable-radius rolling-ball blends were examined by Chuang and Hwang [5].

Cyclides were also used in some simple cases of surface blending. Surface blending using cyclides was studied by Allen and Dutta [6] et al. In addition, Roach and Martin suggested the use of Fourier methods for the generation of blends [7]. Kim and Elber presented a symbolic approach for the computation of blending surfaces [8].

The partial differential equation (PDE)-based method regards surface blending as a boundary value problem. The boundaries of the blending region together with some of their derivatives are combined with a fourth-order PDE to give the mathematical representation of a blending surface [9]. In order to solve the PDEs, some methods such as the finite element method [10], the finite difference method [11], and the collocation method [12], have been developed. Since the vector-valued parameter of the PDE strongly affects the shape of blending

*Corresponding author. Tel.: +44-1202-595055; fax: +44-1202-595530.

E-mail address: jzhang@bournemouth.ac.uk (J.J. Zhang).

surfaces, a more general fourth-order PDE was proposed which has three vector-valued parameters and is more effective in shape manipulation [13].

The above methods deal with blending surfaces with tangential continuity. However, blends with curvature or higher order continuity are often required in practical engineering applications such as the design of the streamlined surfaces of aircraft, ships and cars. Due to the complexity of surface blending with curvature continuity, few publications can be found on this topic. Blends with curvature continuity were examined by Pegna and Wolter [14], Filkins et al. [15] and Schichtel [16].

More recently, a sixth-order PDE with one parameter was used for shape parametrisation of fluid membranes and vesicles. This PDE can be solved by a Fourier series method [17] or a pseudo-spectral method [18]. Both methods suffer from the setback that their accuracy is less satisfactory and difficult to improve by increasing the number of terms of the Fourier series. They are efficient only when a small number of terms are involved. Therefore, developing an efficient and effective resolution method to solve sixth-order PDEs for surface blending remains an unresolved problem.

In this paper, we will propose to use a general sixth-order PDE and develop a fast and accurate solution method for surface blending with C^2 continuity.

2. The sixth-order PDE and its boundary conditions

Compared to the commonly used purely geometric modelling method, the PDE-based modelling methods have the following advantages:

- PDE-based modelling methods are physically based. A fourth-order PDE can be derived from the theory of bending thin elastic plates. Thus the coefficients of such a PDE are closely related to the physical properties of the surface that it represents.
- PDE modelling methods provide alternative means to the control-point based techniques, such as NURBS [19]. The surface shape can be manipulated by changing only a few vector-valued shape parameters or the force function of the PDE or by altering the position, the tangent and the curvature of the boundary conditions of the PDE. The effects that these factors have on the shape of the modelled surface were discussed in [13].

A fourth-order PDE can only meet position and tangent continuities since there are four degrees of freedom in the solution of the PDE. When both curvature and tangent continuities between the primary surfaces and the blending surface are required, a sixth-order PDE must be used. In addition, a sixth-order PDE

provides us with more shape controls, i.e. one more vector-valued shape parameter and two more boundary curvatures. Therefore, a sixth-order PDE is more powerful than a fourth-order PDE in surface manipulation. Due to these reasons, a general sixth-order PDE will be presented below to tackle the blending problems of curvature continuity.

Using a vector operator defined in Eq. (5), we are currently proposing to use a sixth-order PDE with four vector-valued parameters that has the form:

$$\mathbf{a} \frac{\partial^6 \mathbf{x}}{\partial u^6} + \mathbf{b} \frac{\partial^6 \mathbf{x}}{\partial u^4 \partial v^2} + \mathbf{c} \frac{\partial^6 \mathbf{x}}{\partial u^2 \partial v^4} + \mathbf{d} \frac{\partial^6 \mathbf{x}}{\partial v^6} = 0, \quad (1)$$

where $\mathbf{a} = [a_x \ a_y \ a_z]^T$, $\mathbf{b} = [b_x \ b_y \ b_z]^T$, $\mathbf{c} = [c_x \ c_y \ c_z]^T$, $\mathbf{d} = [d_x \ d_y \ d_z]^T$ are the vector-valued parameters, and $\mathbf{x} = [x \ y \ z]^T$ is a vector-valued positional function.

Since the boundary curves of a surface-blending operation are trimlines on the primary surfaces, if we require the blending surface to exhibit tangential continuity with the primary surfaces, the first derivatives of the primary surfaces at the boundary curves need to be known. Given a boundary curve with regular parameterisation (i.e. arc length parameterisation [19]), to achieve curvature continuity, according to Pegna and Wolter [14], the second fundamental form [19] of the blending surface should be equal to those of the primary surfaces at the boundary curves, i.e.,

$$(\mathbf{n} \cdot \mathbf{x}_{uu} du^2 + 2\mathbf{n} \cdot \mathbf{x}_{uv} du dv + \mathbf{n} \cdot \mathbf{x}_{vv} dv^2)_+ \\ = (\mathbf{n} \cdot \mathbf{x}_{uu} du^2 + 2\mathbf{n} \cdot \mathbf{x}_{uv} du dv + \mathbf{n} \cdot \mathbf{x}_{vv} dv^2)_-, \quad (2)$$

where subscripts “+” and “-” denote the blending surface and the primary surface, respectively, and \mathbf{n} is the unit normal vector of the primary surface at the boundary curve.

Eq. (2) can be satisfied when all the second partial derivatives of the blending surface and the primary surfaces at the boundary curves are equal. Therefore, the curvature continuity condition given by Eq. (2) is guaranteed if

$$(\mathbf{x}_{uu})_+ = (\mathbf{x}_{uu})_-, \\ (\mathbf{x}_{uv})_+ = (\mathbf{x}_{uv})_-, \\ (\mathbf{x}_{vv})_+ = (\mathbf{x}_{vv})_-. \quad (3)$$

When considering the positional and tangential continuities of the blending surface and the corresponding primary surface along their boundary curve, curvature continuity can be described by only the first equality of Eq. (3). This can be demonstrated as follows. Assuming that at the boundary curves the position function and the first partial derivative with respect to the parametric variable u are $[\mathbf{x}(v)]_+ = \mathbf{G}_1(v)$ and $[\mathbf{x}_u(v)]_+ = \mathbf{G}_2(v)$ for the blending surface, and the $[\mathbf{x}(v)]_- = \tilde{\mathbf{G}}_1(v)$ and $[\mathbf{x}_u(v)]_- = \tilde{\mathbf{G}}_2(v)$ for the corresponding primary surface, the positional and tangential continuities along the boundary curve require that

$\mathbf{G}_1(v) = \tilde{\mathbf{G}}_1(v)$ and $\mathbf{G}_2(v) = \tilde{\mathbf{G}}_2(v)$. Since $(\mathbf{x}_{vv})_+ = \mathbf{G}_1''(v)$ and $(\mathbf{x}_{uv})_+ = \mathbf{G}_2''(v)$, and $(\mathbf{x}_{vv})_- = \tilde{\mathbf{G}}_1'(v)$ and $(\mathbf{x}_{uv})_- = \tilde{\mathbf{G}}_2'(v)$, we have $(\mathbf{x}_{uv})_+ = (\mathbf{x}_{uv})_-$ and $(\mathbf{x}_{vv})_+ = (\mathbf{x}_{vv})_-$.

After the above treatment, the blending surface that exhibits positional, tangential and curvature continuities at the boundary curve requires the following boundary conditions

$$\begin{aligned} u=0: \\ \mathbf{x} &= \mathbf{G}_1(v), \quad \mathbf{x}_u = \mathbf{G}_2(v), \quad \mathbf{x}_{uu} = \mathbf{G}_3(v), \\ u=1: \\ \mathbf{x} &= \mathbf{G}_4(v), \quad \mathbf{x}_u = \mathbf{G}_5(v), \quad \mathbf{x}_{uu} = \mathbf{G}_6(v). \end{aligned} \quad (4)$$

In fact, as far as curvature continuity is concerned, the boundary conditions given in Eq. (4) are stronger than those given in Eq. (2). Thus, the blend defined with Eq. (4) is C^2 continuous.

In general, boundary conditions (4) is a combination of elementary functions in mathematics including power functions, exponent functions, trigonometric functions, etc. Depending on the blending tasks, the boundary conditions may be simple or complex. For complex boundary conditions, the closed-form solution of PDE (1) may not exist. In such a case, we first transform the boundary conditions into a simpler form.

To facilitate description, we define a vector operator as follows:

$$\mathbf{rs} = [r_x \ r_y \ r_z]^T [s_x \ s_y \ s_z]^T = [r_x s_x \ r_y s_y \ r_z s_z]^T. \quad (5)$$

Then we define basis functions as linearly independent combinations of elementary functions through various mathematical operations but excluding polynomial forms, since a polynomial can be decomposed into a number of basis functions with the form of $a_n v^n$. For example, $v^2/v \cos v$, $e^{\sin v+v}$ and $\ln(v^3+e^v)$ are basis functions, but $a^v + v^2$ and $\cos(v+a^v) - \ln v$ are not.

According to the above definitions, we decompose the functions in Eq. (4) into a number of basis functions and write the boundary conditions (4) into the following forms:

$$\begin{aligned} u=0: \\ \mathbf{x} &= \sum_{i=1}^I \mathbf{d}_{1i} \mathbf{g}_i(v), \quad \mathbf{x}_u = \sum_{i=1}^I \mathbf{d}_{2i} \mathbf{g}_i(v), \quad \mathbf{x}_{uu} = \sum_{i=1}^I \mathbf{d}_{3i} \mathbf{g}_i(v), \\ u=1: \\ \mathbf{x} &= \sum_{i=1}^I \mathbf{d}_{4i} \mathbf{g}_i(v), \quad \mathbf{x}_u = \sum_{i=1}^I \mathbf{d}_{5i} \mathbf{g}_i(v), \quad \mathbf{x}_{uu} = \sum_{i=1}^I \mathbf{d}_{6i} \mathbf{g}_i(v), \end{aligned} \quad (6)$$

where \mathbf{d}_{ji} ($j = 1, 2, \dots, 6$; $i = 1, 2, \dots, I$) are the known constants, $\mathbf{g}_i(v)$ ($i = 1, 2, \dots, I$) are basis functions.

Taking the x component as an example, if the corresponding boundary conditions of the Eq. (4) have

the following forms,

$$u=0:$$

$$x = 5 \sin v + v, \quad x_u = 2 \cos v, \quad x_{uu} = 0,$$

$$u=1:$$

$$x = \frac{7v}{e^v + \ln v}, \quad x_u = 0, \quad x_{uu} = 3v^2 \sinh^{-1} v - 5 \cosh v,$$

the basis functions are $g_{x1}(v) = \sin v$, $g_{x2}(v) = v$, $g_{x3}(v) = \cos v$, $g_{x4}(v) = \frac{v}{e^v + \ln v}$, $g_{x5}(v) = v^2 \sinh^{-1} v$, $g_{x6}(v) = \cosh v$, the boundary conditions for the x component are transformed into:

$$u=0:$$

$$x = 5g_{x1}(v) + g_{x2}(v) + \sum_{i=3}^6 [0 \times g_{xi}(v)],$$

$$x_u = 2g_{x3}(v) + \sum_{\substack{i=1 \\ (i \neq 3)}}^6 [0 \times g_{xi}(v)],$$

$$x_{uu} = \sum_{i=1}^6 [0 \times g_{xi}(v)],$$

$$u=1:$$

$$x = 7g_{x4}(v) + \sum_{\substack{i=1 \\ (i \neq 4)}}^6 [0 \times g_{xi}(v)],$$

$$x_u = \sum_{i=1}^6 [0 \times g_{xi}(v)],$$

$$x_{uu} = 3g_{x5}(v) - 5g_{x6}(v) + \sum_{i=1}^4 [0 \times g_{xi}(v)].$$

After such a transformation, the solution of PDE (1) subjected to the boundary conditions (4) is transformed into the resolution of PDE (1) subject to each of the basis functions. Then, the superimposition of the solutions of PDE (1) under each of the basis functions gives the total solution of PDE (1) subjected to the boundary conditions (4) which represents a blending surface whose boundary curves, tangents and curvatures are defined by the primary surfaces. Such a treatment brings in two advantages. One is that the closed-form solutions of PDE (1) can be achieved for some basis functions subject to which PDE (1) has a closed-form solution. The other is that the solution function of PDE (1) under each of the basis functions is much simpler than that of PDE (1) subject to the total boundary conditions (4). Therefore, it can be better approximated with a proper trial function as discussed below.

3. The compound function and its resolution method

For arbitrary vector-valued parameters, the closed-form solution of PDE (1) under the boundary conditions (6) may not exist or may be difficult to obtain.

Numerical methods, such as the finite element method and the finite difference method, are effective in dealing with such cases. However, these methods are computationally expensive and unsuitable for interactive applications. In this paper, we will develop a semi-analytical method in order to achieve high computational efficiency and accuracy. To this end, a compound function is constructed below:

$$\mathbf{x} = \sum_{i=1}^I \left[\mathbf{a}_{i0} + \sum_{m=1}^M (\mathbf{a}_{im} \cos m\pi u + \mathbf{b}_{im} \sin m\pi u) \right] \mathbf{g}_i(v). \quad (7)$$

In order to meet the boundary conditions (6) exactly, the above compound function (7) is substituted into the boundary conditions (6). Since the basis functions are linearly independent of each other, the following linear algebraic equations are obtained:

$$u = 0 :$$

$$\begin{aligned} \mathbf{a}_{i0} + \sum_{m=1}^M \mathbf{a}_{im} &= \mathbf{d}_{1i}, & \pi \sum_{m=1}^M m \mathbf{b}_{im} &= \mathbf{d}_{2i}, \\ -\pi^2 \sum_{m=1}^M m^2 \mathbf{a}_{im} &= \mathbf{d}_{3i}, \end{aligned}$$

$$u = 1 :$$

$$\begin{aligned} \mathbf{a}_{i0} + \sum_{m=1}^M (-1)^m \mathbf{a}_{im} &= \mathbf{d}_{4i}, & \pi \sum_{m=1}^M (-1)^m m \mathbf{b}_{im} &= \mathbf{d}_{5i}, \\ -\pi^2 \sum_{m=1}^M (-1)^m m^2 \mathbf{a}_{im} &= \mathbf{d}_{6i} \quad (i = 1, 2, \dots, I). \end{aligned} \quad (8)$$

Solving the above six equations for the six unknown constants \mathbf{a}_{i0} , \mathbf{a}_{i1} , \mathbf{a}_{i2} , \mathbf{a}_{i3} , \mathbf{b}_{i1} and \mathbf{b}_{i2} , their mathematical formulae are determined. Then, substituting these constants into (7), the compound function (7) is transformed into the following form:

$$\begin{aligned} \mathbf{x} = \sum_{i=1}^I & [\mathbf{A}_{i01} + \mathbf{A}_{i11} \cos \pi u + \mathbf{A}_{i21} \cos 2\pi u \\ & + \mathbf{A}_{i31} \cos 3\pi u + \sum_{m=4}^M (\mathbf{A}_{i0m} + \mathbf{A}_{i1m} \cos \pi u \\ & + \mathbf{A}_{i2m} \cos 2\pi u + \mathbf{A}_{i3m} \cos 3\pi u + \cos m\pi u) \mathbf{a}_{im} \\ & + \mathbf{B}_{i11} \sin \pi u + \mathbf{B}_{i21} \sin 2\pi u \\ & + \sum_{m=3}^M (\mathbf{B}_{i1m} \sin \pi u + \mathbf{B}_{i2m} \sin 2\pi u + \sin m\pi u) \mathbf{b}_{im}] \mathbf{g}_i(v), \end{aligned} \quad (9)$$

where $\mathbf{A}_{ij1}(i = 1, 2, \dots, I; j = 0, 1, 2, 3)$, $\mathbf{B}_{ij1}(i = 1, 2, \dots, I; j = 1, 2)$, $\mathbf{A}_{ijn}(i = 1, 2, \dots, I; j = 0, 1, 2, 3; m = 4, 5, \dots, M)$ and $\mathbf{B}_{ijn}(i = 1, 2, \dots, I; j = 1, 2; m = 3, 4, \dots, M)$ are given in Appendix A.

In order to determine the remaining unknown constants in the compound functions (9), we here introduce two strategies.

For the basis functions whose second-, fourth- and sixth-order partial derivatives can be expressed by the basis functions themselves, we have:

$$\begin{aligned} \mathbf{g}_i^{(2)}(v) &= e_{i2} \mathbf{g}_i(v), \\ \mathbf{g}_i^{(4)}(v) &= e_{i4} \mathbf{g}_i(v), \\ \mathbf{g}_i^{(6)}(v) &= e_{i6} \mathbf{g}_i(v), \end{aligned} \quad (10)$$

where $\mathbf{g}_i^{(k)}(v) = \frac{d^k \mathbf{g}_i(v)}{dv^k}$ ($k = 2, 4, 6$), and e_{ik} ($i = 1, 2, \dots, I; k = 2, 4, 6$) are known constants generated by differential operations.

Since the compound function (9) is not the accurate solution of PDE (1) under the boundary conditions (6), PDE (1) cannot be exactly met after the introduction of Eq. (9) and an error exists. However, this error can be minimised by substituting the compound function (9) into PDE (1) and equating the terms with the same boundary basis functions. For each of the basis functions, an error function called the residual function is generated by:

$$\begin{aligned} \mathbf{R}_i = \sum_{m=4}^M \tilde{\mathbf{K}}_i(u, m) \mathbf{a}_{im} + \sum_{m=3}^M \hat{\mathbf{K}}_i(u, m) \mathbf{b}_{im} + \mathbf{F}_i(u) \\ (i = 1, 2, \dots, I), \end{aligned} \quad (11)$$

where the known functions $\tilde{\mathbf{K}}_i(u, m)$, $\hat{\mathbf{K}}_i(u, m)$ and $\mathbf{F}_i(u)$ are given in Appendix B.

Alternatively, for the basis functions whose second-, fourth- and sixth-order partial derivatives cannot be expressed by the basis functions themselves, the residual function \mathbf{R}_i can also be obtained below by substituting the above compound function (9) into PDE (1).

$$\begin{aligned} \mathbf{R}_i = \sum_{m=4}^M \tilde{\mathbf{K}}_i(u, v, m) \mathbf{a}_{im} + \sum_{m=3}^M \hat{\mathbf{K}}_i(u, v, m) \mathbf{b}_{im} + \mathbf{F}_i(u, v) \\ (i = 1, 2, \dots, I), \end{aligned} \quad (12)$$

where the known functions $\tilde{\mathbf{K}}_i(u, v, m)$, $\hat{\mathbf{K}}_i(u, v, m)$ and $\mathbf{F}_i(u, v)$ are given in Appendix C.

For the former set of functions (11), we generate $(2M - 5)$ uniformly distributed collocation points within the resolution region $0 \leq u \leq 1$, and set the residual values of the function \mathbf{R}_i at these collocation points to zero, i.e.:

$$\sum_{m=4}^M \tilde{\mathbf{K}}_i(u_l, m) \mathbf{a}_{im} + \sum_{m=3}^M \hat{\mathbf{K}}_i(u_l, m) \mathbf{b}_{im} + \mathbf{F}_i(u_l) = 0,$$

where ($l = 1, 2, \dots, 2M - 5$).

For the latter set of functions (12), $(2M - 5)$ uniformly distributed collocation points are also chosen within the resolution region $\{0 \leq u \leq 1; v_0 \leq v \leq v_1\}$, and the residual values of the function \mathbf{R}_i at these collocation

points are also set to zero, i.e.:

$$\sum_{m=4}^M \tilde{\mathbf{K}}_i(u_l, v_l, m) \mathbf{a}_{im} + \sum_{m=3}^M \hat{\mathbf{K}}_i(u_l, v_l, m) \mathbf{b}_{im} + \mathbf{F}_i(u_l, v_l) = 0,$$

where $l = 1, 2, \dots, (2M - 5)$.

For each component of the position vector \mathbf{x} , each collocation point yields a linear algebraic equation. Writing the equations for all the collocation points in a matrix form, the resolution equations for each of the x , y and z components are obtained as follows [20]:

$$\mathbf{K}_{ji} \mathbf{A}_{ji} = \tilde{\mathbf{F}}_{ji} \quad (13)$$

($j = x, y, z$; $i = 1, 2, \dots, I$),

where \mathbf{K}_{ji} is a square matrix of size $(2M - 5) \times (2M - 5)$, \mathbf{A}_{ji} is a column vector of size $(2M - 5)$, consisting of the unknown constants \mathbf{a}_j ($j = 4, 5, \dots, M$) and \mathbf{b}_j ($j = 3, 4, \dots, M$), and $\tilde{\mathbf{F}}_{ji}$ is a column vector of size $(2M - 5)$ consisting of the known constants. The elements of \mathbf{K}_{ji} , \mathbf{A}_{ji} and $\tilde{\mathbf{F}}_{ji}$ are given in Appendix D.

Using the algorithms for the resolution of linear algebraic equations and the corresponding computer programs given in [21] to solve Eq. (13), we obtain the position functions of the blending surface. When the number of the unknown constants is large, the method given in [22] can be employed to speed up the resolution of Eq. (13).

4. Accuracy and efficiency

The compound function (9) satisfies exactly the boundary conditions (6) and also the residual error on the blending surfaces is minimised. Therefore, our method has a high computational accuracy. In addition, since only a few unknown constants are involved, it is very efficient. In order to justify these statements, here we investigate the accuracy and efficiency of our method.

In order to obtain a closed-form solution, we specifically set the vector-valued parameters to $a_x = a_y = a_z = 1$, $b_x = b_y = b_z = 4$, $c_x = c_y = c_z = -9$, and $d_x = d_y = d_z = -36$. As an example, let us assume that we wish to generate a blending surface between an elliptical cylinder and a circular cylinder. The boundary conditions for this blending task can be written as

$$u = 0 :$$

$$x = a \sin v, \quad \frac{\partial x}{\partial u} = 0, \quad \frac{\partial^2 x}{\partial u^2} = 0,$$

$$y = b \cos v, \quad \frac{\partial y}{\partial u} = 0, \quad \frac{\partial^2 y}{\partial u^2} = 0,$$

$$z = h_1, \quad \frac{\partial z}{\partial u} = -4, \quad \frac{\partial^2 z}{\partial u^2} = 2,$$

$$u = 1 :$$

$$x = r \sin v, \quad \frac{\partial x}{\partial u} = 0, \quad \frac{\partial^2 x}{\partial u^2} = 0,$$

$$y = r \cos v, \quad \frac{\partial y}{\partial u} = 0, \quad \frac{\partial^2 y}{\partial u^2} = 0,$$

$$z = 0, \quad \frac{\partial z}{\partial u} = -4, \quad \frac{\partial^2 z}{\partial u^2} = -2. \quad (14)$$

Here and thereafter, all undefined symbols in the boundary conditions are geometric parameters controlling the boundary curves, tangents and curvatures.

With the above vector-valued parameters and boundary conditions, the closed-form solution of PDE (1) is

$$x = (b_1 e^{2u} + b_2 e^{-2u} + b_3 e^{\sqrt{3}u} + b_4 e^{-\sqrt{3}u} + b_5 \sin \sqrt{3}u + b_6 \cos \sqrt{3}u) \sin v,$$

$$y = (c_1 e^{2u} + c_2 e^{-2u} + c_3 e^{\sqrt{3}u} + c_4 e^{-\sqrt{3}u} + c_5 \sin \sqrt{3}u + c_6 \cos \sqrt{3}u) \cos v,$$

$$z = d_0 + d_1 u + d_2 u^2 + d_3 u^3 + d_4 u^4 + d_5 u^5, \quad (15)$$

where all unknown constants are determined by substituting the above closed-form solution into the boundary conditions (14).

Setting the geometric parameters in Eq. (14) to: $a = 1.6$, $b = r = 1$, and using Eq. (15), we have generated the blending surface shown in Fig. 1a.

Using the boundary conditions (14) and PDE (1), it is very easy to obtain an accurate solution of the z component of Eq. (15). Therefore, when using our method, we only consider the x and y components. The compound functions for this blending task can be

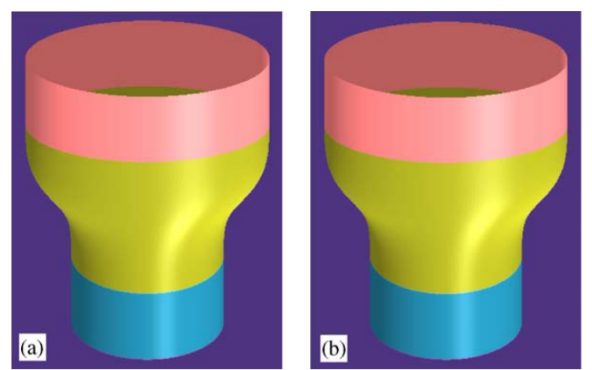


Fig. 1. Comparison between our solution and the closed-form solution.

written as

$$\begin{aligned} x &= \left[a_{x10} + \sum_{m=1}^M (a_{x1m} \cos m\pi u + b_{x1m} \sin m\pi u) \right] \sin v, \\ y &= \left[a_{y10} + \sum_{m=1}^M (a_{y1m} \cos m\pi u + b_{y1m} \sin m\pi u) \right] \cos v. \end{aligned} \quad (16)$$

According to the boundary conditions (14) and the vector-valued basis function $\mathbf{g}_1(v) = [\sin v \cos v 1]^T$, the known constants in Eq. (6) are given by: $\mathbf{d}_{11} = [a \ b \ h_1]^T$, $\mathbf{d}_{21} = [0 \ 0 \ -4]^T$, $\mathbf{d}_{31} = [0 \ 0 \ 2]^T$, $\mathbf{d}_{41} = [r \ r \ 0]^T$, $\mathbf{d}_{51} = [0 \ 0 \ -4]^T$ and $\mathbf{d}_{61} = [0 \ 0 \ -2]^T$. Substituting these known constants and Eq. (16) into Eq. (8), we determine the unknown constants $\mathbf{a}_{l1m}(l = x, y; m = 0, 1, 2, 3)$ and $\mathbf{b}_{l1m}(l = x, y; m = 1, 2)$. Then with Eq. (11), we obtain the residual function of PDE (1) and determine the remaining unknown constants using Eq. (13). Using the same geometric parameters and vector-valued parameters, and taking the number of terms of the Fourier series (16) to be $M = 5$, we have generated the blending surface in Fig. 1b.

Visual inspection of these figures reveals no noticeable difference between the two blending surfaces. In order to quantify their accuracy, we introduce the following error formula which measures the average relative error of two surfaces at a set of chosen points:

$$\begin{aligned} E = & \frac{1}{I_u \times J_v} \sum_{i=1}^{I_u} \sum_{j=1}^{J_v} \{ \{ [x(u_i, v_j) - \tilde{x}(u_i, v_j)]^2 \\ & + [y(u_i, v_j) - \tilde{y}(u_i, v_j)]^2 \\ & + [z(u_i, v_j) - \tilde{z}(u_i, v_j)]^2 \}^{1/2} / \{ [x(u_i, v_j)]^2 \\ & + [y(u_i, v_j)]^2 + [z(u_i, v_j)]^2 \}^{1/2} \}, \end{aligned} \quad (17)$$

where x, y, z represent the components derived by the closed-form solutions and $\tilde{x}, \tilde{y}, \tilde{z}$ represent the components derived by our method and where I_u and J_v represent the number of the chosen points along the u and v parametric directions, respectively.

On the surfaces generated by each of these solutions, we have uniformly collocated 100 points along the u and v directions ($I_u = J_v = 100$), i.e. 10^4 points were collocated on each surface. In order to investigate the convergence of the Fourier series (16), we set the number of terms of the Fourier series to be, $M = 4, 5$ and 8 , and using Eq. (17) we calculated the average relative errors between the two generated surfaces and listed the results in Table 1. In this Table, E represents the average relative error calculated with Eq. (17), and T indicates the time used to determine the unknown constants in the solutions of all three components.

The error between our solution and the closed-form solution is very small even when very few Fourier series terms were used, i.e. $M = 4$. Furthermore, our solution

Table 1
Errors and computation times of the proposed method

M	E	T (s)
4	7.01×10^{-2}	$<10^{-6}$
5	1.08×10^{-3}	$<10^{-6}$
8	5.22×10^{-4}	$<10^{-6}$

method converged quickly when more terms were used. For the following examples where the closed-form solution exists, our proposed method and the closed-form solution also generated almost identical blending surfaces. In addition to its good accuracy, our method is also very efficient. For the closed-form solution, the time taken to determine the unknown constants of Eq. (15) is less than 10^{-6} of a second on an 800 MHz PC. This is so in the three cases. Therefore, we can conclude that our method can produce blending surfaces almost as accurately and as fast as the closed-form solution method. Furthermore, our method can solve complex blending problems which cannot be tackled with the closed-form resolution method.

We have also compared our method with the Fourier series method and the pseudo-spectral method. In order to save space, the details of the comparison will not be given here. The result indicates that the method proposed in this paper is more accurate and efficient than both methods.

5. Example applications

In this section, we give some examples to demonstrate the application of our method to a variety of surface-blending problems. We will also examine the effects of the vector-valued parameters and the geometric parameters on the shape of the blending surface.

In our first example, the parametric form of the boundary conditions defined by the elliptical cylinder and the ellipsoid can be written as:

$$u = 0 :$$

$$x = a \cos v, \quad \frac{\partial x}{\partial u} = 0, \quad \frac{\partial^2 x}{\partial u^2} = 0,$$

$$y = b \sin v, \quad \frac{\partial y}{\partial u} = 0, \quad \frac{\partial^2 y}{\partial u^2} = 0,$$

$$z = h_0 - h_1, \quad \frac{\partial z}{\partial u} = -2h_1, \quad \frac{\partial^2 z}{\partial u^2} = -2h_1,$$

$$u = 1 :$$

$$x = c \sin 0.3\pi \cos v, \quad \frac{\partial x}{\partial u} = c \cos 0.3\pi \cos v,$$

$$\frac{\partial^2 x}{\partial u^2} = -c \sin 0.3\pi \cos v,$$

$$\begin{aligned}
y &= d \sin 0.3\pi \sin v, \quad \frac{\partial y}{\partial u} = d \cos 0.3\pi \sin v, \\
\frac{\partial^2 y}{\partial u^2} &= -d \sin 0.3\pi \sin v, \\
z &= h_2 + h_3 \cos 0.3\pi, \quad \frac{\partial z}{\partial u} = -h_3 \sin 0.3\pi, \\
\frac{\partial^2 z}{\partial u^2} &= -h_3 \cos 0.3\pi.
\end{aligned} \tag{18}$$

In the resolution region $0 \leq u \leq 1$, we uniformly distribute 15 collocation points. For each of these points, Eqs. (13) are derived and solved for the unknown constants \mathbf{a}_{ij} ($j = 4, 5, \dots, 10$) and \mathbf{b}_{ij} ($j = 3, 4, \dots, 10$). First by setting the geometric parameters in boundary conditions (18) to: $a = d = 1.2$, $b = 0.8$, $c = 2$, $h_0 = 3$, $h_1 = 1$, $h_2 = -0.3$, $h_3 = 0.8$ and all the vector-valued parameters to 1, we obtain the blending surface shown in Fig. 2a. Fig. 2b shows the same surfaces as Fig. 2a rendered with the same colour. Observe that in Fig. 2b the three surfaces blend smoothly and it is impossible to detect the boundary curves between the primary surfaces and the blending surface. This indicates that we have achieved both tangent and curvature continuity between the surfaces. When the vector-valued parameter is changed to $d_x = d_y = -8000$, the blending surface shown in Fig. 2c is generated. It is clear that varying the vector-valued parameter changes the shape of the blending surface, while the continuity between the blending surface and the primary surfaces remains unaffected.

In our second example, we examine the blending surface between a circular torus and an elliptic hyperboloid. The boundary conditions for this blending problem are:

$$\begin{aligned}
u &= 0 : \\
x &= (R + A \cos u_0) \cos v, \quad \frac{\partial x}{\partial u} = -A \sin u_0 \cos v, \\
\frac{\partial^2 x}{\partial u^2} &= -A \cos u_0 \cos v, \\
y &= (R + A \cos u_0) \sin v, \quad \frac{\partial y}{\partial u} = -A \sin u_0 \sin v,
\end{aligned}$$

$$\begin{aligned}
\frac{\partial^2 y}{\partial u^2} &= -A \cos u_0 \sin v, \\
z &= A \sin u_0, \quad \frac{\partial z}{\partial u} = A \cos u_0, \quad \frac{\partial^2 z}{\partial u^2} = -A \sin u_0, \\
u &= 1 : \\
x &= a \cosh u_1 \cos v, \quad \frac{\partial x}{\partial u} = a \sinh u_1 \cos v, \\
\frac{\partial^2 x}{\partial u^2} &= a \cosh u_1 \cos v, \\
y &= b \cosh u_1 \sin v, \quad \frac{\partial y}{\partial u} = b \sinh u_1 \sin v, \\
\frac{\partial^2 y}{\partial u^2} &= b \cosh u_1 \sin v, \\
z &= h_0 + h_1 \sinh u_1, \quad \frac{\partial z}{\partial u} = h_1 \cosh u_1, \\
\frac{\partial^2 z}{\partial u^2} &= h_1 \sinh u_1.
\end{aligned} \tag{19}$$

Similar to the previous example, we uniformly distribute 15 collocation points and set the geometric parameters to: $a = h_1 = 1$, $b = 0.7$, $h_0 = -1.6$, $R = 1.7$, $A = 0.3$, and all vector-valued parameters to 1. The positions of the boundary curves are taken to be at: $u_0 = 1.7\pi$ and $u_1 = 0$. The blending surface obtained is depicted in Fig. 3a. Then we change the geometric parameter a to 0.5 and we obtain the blending surface shown in Fig. 3b. Varying any of the geometric parameters has a significant effect on the shape of the blending surface.

Finally, let us present three more complex surface-blending examples. The first is to blend two conic frustums: one has many wrinkles on its surface and the other has a circular cross section. The boundary conditions for this blending problem are

$$\begin{aligned}
u &= 0 : \\
x &= 0.6 \cos v, \quad \frac{\partial x}{\partial u} = 0, \quad \frac{\partial^2 x}{\partial u^2} = 0, \\
y &= 0.6 \sin v, \quad \frac{\partial y}{\partial u} = 0, \quad \frac{\partial^2 y}{\partial u^2} = 0,
\end{aligned}$$

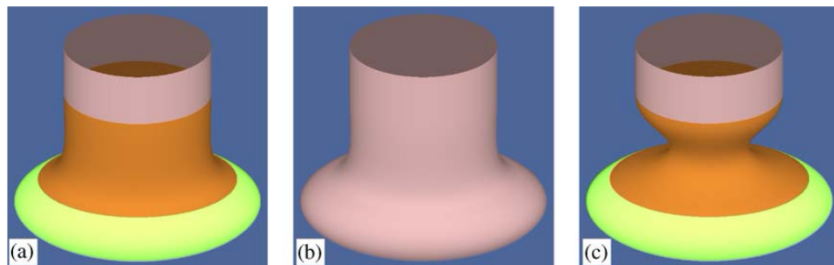


Fig. 2. Blending between an elliptical cylinder and an ellipsoid.

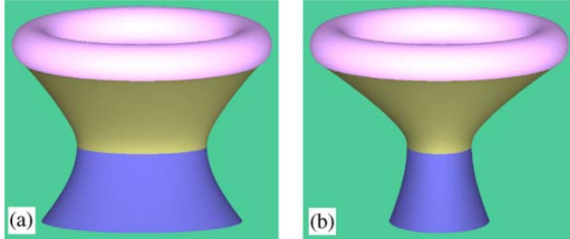


Fig. 3. Blending between a circular torus and an elliptic hyperboloid.

$$\begin{aligned}
 z &= -1.2, \quad \frac{\partial z}{\partial u} = 1.5, \quad \frac{\partial^2 z}{\partial u^2} = 0, \\
 u &= 1 : \\
 x &= 0.909 \cos v + 0.051 \cos(12v), \\
 \frac{\partial x}{\partial u} &= 1.8 \cos v + 0.01 \cos(12v), \\
 \frac{\partial^2 x}{\partial u^2} &= 1.8 \cos v + 0.1 \cos(12v), \\
 y &= 0.909 \sin v + 0.051 \sin(12v), \\
 \frac{\partial y}{\partial u} &= 0.18 \sin v + 0.01 \sin(12v), \\
 \frac{\partial^2 y}{\partial u^2} &= 1.8 \sin v + 0.1 \sin(12v), \\
 z &= 0.45, \quad \frac{\partial z}{\partial u} = 1, \quad \frac{\partial^2 z}{\partial u^2} = 0. \tag{20}
 \end{aligned}$$

The basis functions for the x component are $\cos v$ and $\cos 12v$, and for the y component are $\sin v$ and $\sin 12v$. Taking all the vector-valued parameters to be 1, the number of Fourier series terms to be $M = 5$, and employing the above-proposed method, the obtained blending surface is depicted in Fig. 4.

The second example is to generate a blending surface between the frustum of a declined circular cone and a declined plane at a specified circle. The boundary conditions for this blending task are

$$\begin{aligned}
 u &= 0 : \\
 x &= 1.504 \cos v, \quad \frac{\partial x}{\partial u} = -0.94 \cos v, \quad \frac{\partial^2 x}{\partial u^2} = 0, \\
 y &= 1.6 \sin v, \quad \frac{\partial y}{\partial u} = -\sin v, \quad \frac{\partial^2 y}{\partial u^2} = 0, \\
 z &= -0.547 \cos v, \quad \frac{\partial z}{\partial u} = 0.1 + 0.308 \cos v, \quad \frac{\partial^2 z}{\partial u^2} = 0, \\
 u &= 1 : \\
 x &= 0.648 \cos v, \quad \frac{\partial x}{\partial u} = 1.296 \cos v, \quad \frac{\partial^2 x}{\partial u^2} = 2.16 \cos v, \\
 y &= 0.648 \sin v, \quad \frac{\partial y}{\partial u} = 1.296 \sin v, \quad \frac{\partial^2 y}{\partial u^2} = 2.16 \sin v, \\
 z &= 1.8 + 0.5 \cos v, \quad \frac{\partial z}{\partial u} = 2.5, \quad \frac{\partial^2 z}{\partial u^2} = 0. \tag{21}
 \end{aligned}$$

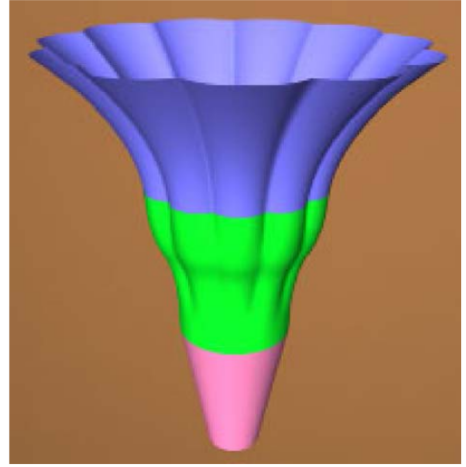


Fig. 4. Blending between a wrinkled surface and a conic surface.

Setting $c_x = c_y = c_z = 100$ and all other vector-valued parameters to 1, the obtained blending surface is shown in Fig. 5.

For all the above examples, when the number of Fourier series terms is set to $M = 5$, the time used to determine all the unknown constants is less than 10^{-6} of one second on an 800 MHz PC.

The last example is to blend between two intersecting cylinders. The boundary conditions guaranteeing the generation of a blending surface with up to C^2 continuity can be written as:

$$\begin{aligned}
 u &= 0 : \\
 x &= s \cos v, \quad \frac{\partial x}{\partial u} = 0, \quad \frac{\partial^2 x}{\partial u^2} = 0, \\
 y &= s \sin v, \quad \frac{\partial y}{\partial u} = 0, \quad \frac{\partial^2 y}{\partial u^2} = 0, \\
 z &= \sqrt{G_1(v)}, \quad \frac{\partial z}{\partial u} = \frac{r + k_1}{\sqrt{G_1(v)}}, \\
 \frac{\partial^2 z}{\partial u^2} &= \frac{1}{\sqrt{G_1(v)}} - \frac{(r + k_1)^2}{\sqrt[3]{G_1(v)}}, \\
 u &= 1 : \\
 x &= (s + l_1) \cos v, \quad \frac{\partial x}{\partial u} = (s + l_1) \cos v, \quad \frac{\partial^2 x}{\partial u^2} = 0, \\
 y &= (s + l_1) \sin v, \quad \frac{\partial y}{\partial u} = (s + l_1) \sin v, \quad \frac{\partial^2 y}{\partial u^2} = 0, \\
 z &= \sqrt{G_2(v)}, \quad \frac{\partial z}{\partial u} = \frac{(s + l_1)\cos^2 v}{\sqrt{G_2(v)}}, \\
 \frac{\partial^2 z}{\partial u^2} &= \frac{\cos^2 v}{\sqrt{G_2(v)}} - \frac{(s + l_1)^2 \cos^4 v}{\sqrt[3]{G_2(v)}}, \tag{22}
 \end{aligned}$$

where $G_1(v) = (r + k_1)^2 - s^2 \cos^2 v$, $G_2(v) = r^2 - (s + l_1)^2 \cos^2 v$, s , l_1 and k_1 are the parameters specifying

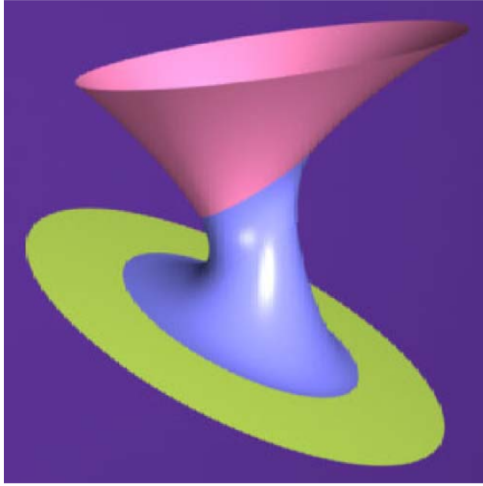


Fig. 5. Blending between the frustum of a declined circular cone and a declined plane.

the trimlines and the first and second derivatives at these trimlines.

The basis function for the x component is $\cos v$, and for the y component is $\sin v$. The basis functions for the z component are $g_{z1}(v) = \sqrt{G_1(v)}$, $g_{z2}(v) = \frac{1}{\sqrt{G_1(v)}}$, $g_{z3}(v) = \frac{1}{\sqrt[3]{G_1(v)}}$, $g_{z4}(v) = \sqrt{G_2(v)}$, $g_{z5}(v) = \frac{\cos^2 v}{\sqrt{G_2(v)}}$ and $g_{z6}(v) = \frac{\cos^4 v}{\sqrt[3]{G_2(v)}}$. Using these basis functions and Eq. (7), the solution of PDE (1) can be expressed in the following form:

$$\begin{aligned} x &= \left[a_{x10} + \sum_{m=1}^M (a_{x1m} \cos m\pi u + b_{x1m} \sin m\pi u) \right] \cos v, \\ y &= \left[a_{y10} + \sum_{m=1}^M (a_{y1m} \cos m\pi u + b_{y1m} \sin m\pi u) \right] \sin v, \\ z &= \sum_{i=1}^6 \left[a_{zi0} + \sum_{m=1}^M (a_{zim} \cos m\pi u + b_{zim} \sin m\pi u) \right] g_{zi}(v). \end{aligned} \quad (23)$$

Using the method developed in this paper, we obtain the residual functions $R_{x1}(u)$ of the x component and $R_{y1}(u)$ of the y component from Eq. (11), and the residual functions $R_{zi}(u)$ ($i = 1, 2, \dots, 6$) of the z component from Eq. (12). Then solving the linear algebraic Eqs. (13), we obtain the solution of PDE (1) subject to the boundary conditions (22). Fig. 6 depicts the generated blending surface between the two intersecting cylinders.

6. Conclusion and future work

In this paper, we have developed a method for the generation of blending surfaces with C^2 continuity using

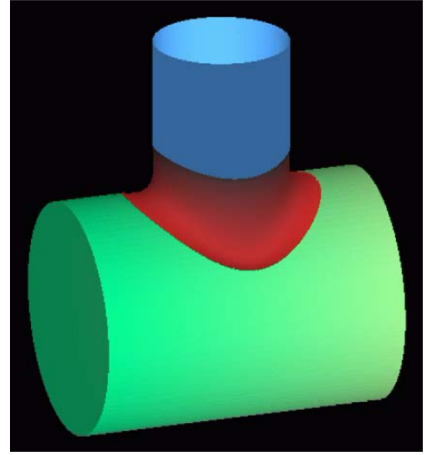


Fig. 6. Blending between two intersecting cylinders.

the solution to a general sixth-order PDE. This PDE has three vector-valued parameters and is more effective in controlling the shape of blending surfaces than the previously published PDE methods.

In order to solve the sixth-order PDE, we construct a compound function which exactly satisfies all the boundary conditions and minimises the error of the PDE. Comparison with the other methods indicates that our method can generate blending surfaces almost as fast and as accurately as the closed-form resolution method, and has higher computational accuracy and efficiency than the existing methods.

The proposed method was applied to some surface-blending examples. The effects of the vector-valued parameters and the geometric parameters on the shape of the blending surface were examined. We have also demonstrated that our method can be used to solve complex surface-blending problems.

As well as being applicable to surface blending, the developed method can also be applied to complex free-form surface generation and manipulation. It is easy to prove that the proposed compound function not only achieves up to C^2 continuity in the u parametric direction, but also can be made to meet the same continuity conditions in the v direction. Making use of this property, the proposed compound function can be employed to construct n -sided patches as well. This is a very useful feature which extends the ability of existing PDE-based surface modelling methods.

In the past some researchers have tried to control the shape of the cross-patch boundaries. For example in [23], the author controls the shape of the surface using three shape parameters, namely: tension, continuity and bias. The method presented in this paper could be refined to generate surfaces with arbitrary cross-patch boundaries simply by changing the first partial derivatives and by removing the second partial derivatives in the boundary conditions. We intend to investigate these issues in future work.

Appendix A. The mathematical expressions of \mathbf{A}_{ij1} , \mathbf{B}_{ij1} , \mathbf{A}_{ijm} and \mathbf{B}_{ijm} are:

$$\mathbf{A}_{i01} = 0.5(\mathbf{d}_{1i} + \mathbf{d}_{4i}) + \frac{1}{8\pi^2}(\mathbf{d}_{3i} + \mathbf{d}_{6i}),$$

$$\mathbf{A}_{i11} = \frac{9}{16}(\mathbf{d}_{1i} - \mathbf{d}_{4i}) + \frac{1}{16\pi^2}(\mathbf{d}_{3i} - \mathbf{d}_{6i}),$$

$$\mathbf{A}_{i21} = -\frac{1}{8\pi^2}(\mathbf{d}_{3i} + \mathbf{d}_{6i}),$$

$$\mathbf{A}_{i31} = \frac{1}{16}(\mathbf{d}_{4i} - \mathbf{d}_{1i}) + \frac{1}{16\pi^2}(\mathbf{d}_{6i} - \mathbf{d}_{3i}),$$

$$\mathbf{B}_{i11} = \frac{1}{2\pi}(\mathbf{d}_{2i} - \mathbf{d}_{5i}),$$

$$\mathbf{B}_{i21} = \frac{1}{4\pi}(\mathbf{d}_{2i} + \mathbf{d}_{5i}),$$

$$\mathbf{A}_{i0m} = \frac{1}{8}[1 + (-1)^m](m^2 - 4),$$

$$\mathbf{A}_{i1m} = \frac{1}{16}[1 - (-1)^m](m^2 - 9),$$

$$\mathbf{A}_{i2m} = -\frac{1}{8}[1 + (-1)^m]m^2,$$

$$\mathbf{A}_{i3m} = -\frac{1}{16}[1 - (-1)^m](m^2 - 1),$$

$$\mathbf{B}_{i1m} = \frac{1}{2}[(-1)^m - 1]m,$$

$$\mathbf{B}_{i2m} = -\frac{1}{4}[(-1)^m + 1]m,$$

where \mathbf{d}_{ji} ($j = 1, 2, \dots, 6$; $i = 1, 2, \dots, I$) are the same as those in Eq. (6).

Appendix B. The mathematical expressions of the known functions $\tilde{\mathbf{K}}_i(u, m)$, $\hat{\mathbf{K}}_i(u, m)$ and $\mathbf{F}_i(u)$ are:

$$\begin{aligned} \tilde{\mathbf{K}}_i(u, m) &= [\tilde{K}_{xi}(u, m) \quad \tilde{K}_{yi}(u, m) \quad \tilde{K}_{zi}(u, m)]^T \\ &= \mathbf{d}\mathbf{A}_{i0m} + \mathbf{C}_{il}\mathbf{A}_{ilm} \cos \pi u + \mathbf{C}_{i2}\mathbf{A}_{i2m} \cos 2\pi u \\ &\quad + \mathbf{C}_{i3}\mathbf{A}_{i3m} \cos 3\pi u + \mathbf{C}_{im} \cos m\pi u \\ &\quad (m = 4, 5, \dots, M), \end{aligned}$$

$$\begin{aligned} \hat{\mathbf{K}}_i(u, m) &= [\hat{K}_{xi}(u, m) \quad \hat{K}_{yi}(u, m) \quad \hat{K}_{zi}(u, m)]^T \\ &= \mathbf{C}_{il}\mathbf{B}_{ilm} \sin \pi u + \mathbf{C}_{i2}\mathbf{B}_{i2m} \sin 2\pi u \\ &\quad + \mathbf{C}_{im} \sin m\pi u \\ &\quad (m = 3, 4, \dots, M), \end{aligned}$$

$$\begin{aligned} \mathbf{F}_i(u) &= [F_{xi}(u) \quad F_{yi}(u) \quad F_{zi}(u)]^T \\ &= \mathbf{d}\mathbf{A}_{i01} + \mathbf{C}_{il}\mathbf{A}_{i11} \cos \pi u + \mathbf{C}_{i2}\mathbf{A}_{i21} \cos 2\pi u \\ &\quad + \mathbf{C}_{i3}\mathbf{A}_{i31} \cos 3\pi u + \mathbf{C}_{il}\mathbf{B}_{i11} \sin \pi u \\ &\quad + \mathbf{C}_{i2}\mathbf{B}_{i21} \sin 2\pi u, \end{aligned}$$

where

$$\mathbf{C}_{im} = -m^6\pi^6\mathbf{a} + m^4\pi^4\mathbf{e}_{i2}\mathbf{b} - m^2\pi^2\mathbf{e}_{i4}\mathbf{c} + \mathbf{e}_{i6}\mathbf{d} \quad (m = 1, 2, \dots, M)$$

and where \mathbf{a} , \mathbf{b} , \mathbf{c} and \mathbf{d} are the vector-valued parameters given in Eq. (1).

Appendix C. The mathematical expressions of the known functions $\tilde{\mathbf{K}}_i(u, v, m)$, $\hat{\mathbf{K}}_i(u, v, m)$ and $\mathbf{F}_i(u, v)$ are:

$$\begin{aligned} \tilde{\mathbf{K}}_i(u, v, m) &= [\tilde{K}_{xi}(u, v, m) \quad \tilde{K}_{yi}(u, v, m) \quad \tilde{K}_{zi}(u, v, m)]^T \\ &= -\pi^6\mathbf{a}(\mathbf{A}_{i1m} \cos \pi u + 64\mathbf{A}_{i2m} \cos 2\pi u \\ &\quad + 729\mathbf{A}_{i3m} \cos 3\pi u + m^6 \cos m\pi u)\mathbf{g}_i(v) \\ &\quad + \pi^4\mathbf{b}(\mathbf{A}_{i1m} \cos \pi u + 16\mathbf{A}_{i2m} \cos 2\pi u \\ &\quad + 81\mathbf{A}_{i3m} \cos 3\pi u + m^4 \cos m\pi u)\mathbf{g}_i^{(2)}(v) \\ &\quad - \pi^2\mathbf{c}(\mathbf{A}_{i1m} \cos \pi u + 4\mathbf{A}_{i2m} \cos 2\pi u \\ &\quad + 9\mathbf{A}_{i3m} \cos 3\pi u + m^2 \cos m\pi u)\mathbf{g}_i^{(4)}(v) \\ &\quad + \mathbf{d}(\mathbf{A}_{i0m} + \mathbf{A}_{i1m} \cos \pi u + \mathbf{A}_{i2m} \cos 2\pi u \\ &\quad + \mathbf{A}_{i3m} \cos 3\pi u + \cos m\pi u)\mathbf{g}_i^{(6)}(v) \\ &\quad (m = 4, 5, \dots, M), \end{aligned}$$

$$\begin{aligned} \hat{\mathbf{K}}_i(u, v, m) &= [\hat{K}_{xi}(u, v, m) \quad \hat{K}_{yi}(u, v, m) \quad \hat{K}_{zi}(u, v, m)]^T \\ &= -\pi^6\mathbf{a}(\mathbf{B}_{i1m} \sin \pi u + 64\mathbf{B}_{i2m} \sin 2\pi u \\ &\quad + m^6 \sin m\pi u)\mathbf{g}_i(v) + \pi^4\mathbf{b}(\mathbf{B}_{i1m} \sin \pi u \\ &\quad + 16\mathbf{B}_{i2m} \sin 2\pi u + m^4 \sin m\pi u)\mathbf{g}_i^{(2)}(v) \\ &\quad - \pi^2\mathbf{c}(\mathbf{B}_{i1m} \sin \pi u + 4\mathbf{B}_{i2m} \sin 2\pi u \\ &\quad + m^2 \sin m\pi u)\mathbf{g}_i^{(4)}(v) + \mathbf{d}(\mathbf{B}_{i1m} \sin \pi u \\ &\quad + \mathbf{B}_{i2m} \sin 2\pi u + \sin m\pi u)\mathbf{g}_i^{(6)}(v) \\ &\quad (m = 3, 4, \dots, M), \end{aligned}$$

$$\begin{aligned} \mathbf{F}_i(u, v) &= [F_{xi}(u, v) \quad F_{yi}(u, v) \quad F_{zi}(u, v)]^T \\ &= -\pi^6\mathbf{a}(\mathbf{A}_{i1} \cos \pi u + 64\mathbf{A}_{i2} \cos 2\pi u \\ &\quad + 729\mathbf{A}_{i3} \cos 3\pi u + \mathbf{B}_{i1} \sin \pi u \\ &\quad + 64\mathbf{B}_{i2} \sin 2\pi u)\mathbf{g}_i(v) + \pi^4\mathbf{b}(\mathbf{A}_{i1} \cos \pi u \\ &\quad + 16\mathbf{A}_{i2} \cos 2\pi u + 81\mathbf{A}_{i3} \cos 3\pi u \\ &\quad + \mathbf{B}_{i1} \sin \pi u + 16\mathbf{B}_{i2} \sin 2\pi u)\mathbf{g}_i^{(2)}(v) \\ &\quad - \pi^2\mathbf{c}(\mathbf{A}_{i1} \cos \pi u + 4\mathbf{A}_{i2} \cos 2\pi u \\ &\quad + 9\mathbf{A}_{i3} \cos 3\pi u + \mathbf{B}_{i1} \sin \pi u \\ &\quad + 4\mathbf{B}_{i2} \sin 2\pi u)\mathbf{g}_i^{(4)}(v) \\ &\quad + \mathbf{d}(\mathbf{A}_{i0} + \mathbf{A}_{i1} \cos \pi u + \mathbf{A}_{i2} \cos 2\pi u \\ &\quad + \mathbf{A}_{i3} \cos 3\pi u + \mathbf{B}_{i1} \sin \pi u \\ &\quad + \mathbf{B}_{i2} \sin 2\pi u)\mathbf{g}_i^{(6)}(v), \end{aligned}$$

where \mathbf{a} , \mathbf{b} , \mathbf{c} and \mathbf{d} are the same as above.

Appendix D. The elements of matrices \mathbf{K}_{ji} , \mathbf{A}_{ji} and $\tilde{\mathbf{F}}_{ji}$

For each component x , y and z of the position vector \mathbf{x} , the elements of Eq. (13) according to Eq. (11) can be

written as

$$K_{ji} = \begin{bmatrix} \tilde{K}_{ji}(u_1, 4) & \tilde{K}_{ji}(u_1, 5) & \cdots & \tilde{K}_{ji}(u_1, M) & \hat{K}_{ji}(u_1, 3) & \hat{K}_{ji}(u_1, 4) & \cdots & \hat{K}_{ji}(u_1, M) \\ \tilde{K}_{ji}(u_2, 4) & \tilde{K}_{ji}(u_2, 5) & \cdots & \tilde{K}_{ji}(u_2, M) & \hat{K}_{ji}(u_2, 3) & \hat{K}_{ji}(u_2, 4) & \cdots & \hat{K}_{ji}(u_2, M) \\ \tilde{K}_{ji}(u_3, 4) & \tilde{K}_{ji}(u_3, 5) & \cdots & \tilde{K}_{ji}(u_3, M) & \hat{K}_{ji}(u_3, 3) & \hat{K}_{ji}(u_3, 4) & \cdots & \hat{K}_{ji}(u_3, M) \\ \tilde{K}_{ji}(u_4, 4) & \tilde{K}_{ji}(u_4, 5) & \cdots & \tilde{K}_{ji}(u_4, M) & \hat{K}_{ji}(u_4, 3) & \hat{K}_{ji}(u_4, 4) & \cdots & \hat{K}_{ji}(u_4, M) \\ \cdots & \cdots \\ \tilde{K}_{ji}(u_{2M-7}, 4) & \tilde{K}_{ji}(u_{2M-7}, 5) & \cdots & \tilde{K}_{ji}(u_{2M-7}, M) & \hat{K}_{ji}(u_{2M-7}, 3) & \hat{K}_{ji}(u_{2M-7}, 4) & \cdots & \hat{K}_{ji}(u_{2M-7}, M) \\ \tilde{K}_{ji}(u_{2M-6}, 4) & \tilde{K}_{ji}(u_{2M-6}, 5) & \cdots & \tilde{K}_{ji}(u_{2M-6}, M) & \hat{K}_{ji}(u_{2M-6}, 3) & \hat{K}_{ji}(u_{2M-6}, 4) & \cdots & \hat{K}_{ji}(u_{2M-6}, M) \\ \tilde{K}_{ji}(u_{2M-5}, 4) & \tilde{K}_{ji}(u_{2M-5}, 5) & \cdots & \tilde{K}_{ji}(u_{2M-5}, M) & \hat{K}_{ji}(u_{2M-5}, 3) & \hat{K}_{ji}(u_{2M-5}, 4) & \cdots & \hat{K}_{ji}(u_{2M-5}, M) \end{bmatrix}$$

$$\mathbf{A}_{ji} = [a_{ji4} \ a_{ji5} \ \cdots \ a_{jiM} \ b_{ji3} \ b_{ji4} \ \cdots \ b_{jiM}]^T$$

$$\bar{\mathbf{F}}_{ji} = [F_{ji}(u_1) \ F_{ji}(u_2) \ \cdots \ F_{ji}(u_{M-3}) \ F_{ji}(u_{M-2}) \ F_{ji}(u_{M-1}) \ \cdots \ F_{ji}(u_{2M-5})]^T$$

$$(j = x, y, z; i = 1, 2, \dots, I).$$

The elements of Eq. (13) according to Eq. (12) also have the same forms as above. However, all the $u_l (l = 1, 2, \dots, 2M - 5)$ should be replaced by $u_l, v_l (l = 1, 2, \dots, 2M - 5)$.

References

- [1] Ohkura K, Kakazu Y. Generalization of the potential method for blending three surfaces. Computer Aided Design 1992;24(11):599–609.
- [2] Rossignac JR, Requicha AAG. Constant-radius blending in solid modeling. Computers in Mechanical Engineering 1984; 65–73.
- [3] Lukács G. Differential geometry of G^1 variable radius rolling ball blend surfaces. Computer Aided Geometric Design 1998;15:585–613.
- [4] Barnhill RE, Farin GE, Chen Q. Constant-radius blending of parametric surfaces. Computing Supplement 1993;8:1–20.
- [5] Chuang JH, Hwang WC. Variable-radius blending by constrained spine generation. The Visual Computer 1997;13:316–29.
- [6] Allen G, Dutta D. Supercyclides and blending. Computer Aided Geometric Design 1997;14:637–51.
- [7] Roach PA, Martin RR. Production of blends and fairings by Fourier methods. SPIE: Curves and Surfaces in Computer Vision and Graphics III 1992;1830:162–73.
- [8] Kim K, Elber G. A symbolic approach to freeform parametric surface blends. The Journal of Visualisation and Computer Animation 1996;8:69–80.
- [9] Bloor MIG, Wilson MJ. Generation blend surfaces using partial differential equations. Computer Aided Design 1989;21(3):165–71.
- [10] Li ZC, Chang CS. Boundary penalty finite element methods for blending surfaces, III, Superconvergence and stability and examples. Journal of Computational and Applied Mathematics 1999;110:241–70.
- [11] You LH, Zhang JJ, Comninou P. Cloth deformation modelling using a plate bending model. In: Proceedings of the seventh International Conference in Central Europe on Computer Graphics, Visualisation and Interactive Digital Media, Plzen, Czech Republic, 8–12 February 1999. p. 485–91.
- [12] Bloor MIG, Wilson MJ. Representing PDE surfaces in terms of B-splines. Computer Aided Design 1990;22(6):324–31.
- [13] Zhang JJ, You LH. PDE based surface representation—vase design. Computers & Graphics 2002;26:89–98.
- [14] Pegna J, Wolter FE. Geometrical criteria to guarantee curvature continuity of blend surfaces. Journal of Mechanical Design, Transactions of the ASME 1992;114:201–10.
- [15] Filkins PC, Tuohy ST, Patrikalakis NM. Computational methods for blending surface approximation. Engineering with Computers 1993;9:49–62.
- [16] Schichtel M. G^2 blend surfaces and filling of N-sided holes. IEEE Computer Graphics and Applications 1993(9):68–73.
- [17] Bloor MIG, Wilson MJ. Method for efficient shape parametrization of fluid membranes and vesicles. Physical Review E 2000;61(4):4218–29.
- [18] Bloor MIG, Wilson MJ. Spectral approximations to PDE surfaces. Computer Aided Design 1996;28(2):145–52.
- [19] Farin G. Curves and surfaces for computer aided geometric design: a practical guide, 4th ed. New York: Academic Press; 1997.
- [20] You LH, Zhang JJ, Comninou P. A solid volumetric model of muscle deformation for computer animation using the weighted residual method. Computer Methods in Applied Mechanics and Engineering 2000;190:853–63.
- [21] Press WH, Teukolsky SA, Vetterling WT, Flannery BP. Numerical recipes in C: the art of scientific computing, 2nd ed. Cambridge: Cambridge University Press; 1992.

- [22] Kobbelt L. Discrete fairing. In: Proceedings of the Seventh IMA Conference on the Mathematics of Surfaces; 1997. p. 101–31.
- [23] Comninos P. An interpolating piecewise bicubic surface with shape parameters. *Computers & Graphics* 2001;25:463–81.

